CASE REPORT
Urooncology

Doi: 10.4274/jus.galenos.2025.2024-12-4
J Urol Surg

Metastatic Primary Renal Well-differentiated Neuroendocrine Tumor: Our Experience with Current Treatment and Clinical Management in a Young Female Patient

Uğur Aferin[1], İclal Gürses[2], Engin Dereköylü[3], Göktuğ Kalender[4], Nil Urgancı[5], Bülent Önal[6]

[1]*Florance Nightingale Hospital, T.C. Demiroğlu Bilim University Faculty of Medicine, Department of Urology, İstanbul, Turkiye*
[2]*İstanbul University-Cerrahpaşa, Cerrahpaşa Faculty of Medicine, Department of Pathology, İstanbul, Turkiye*
[3]*Ağrı State Hospital, Clinic of Urology, Ağrı, Turkiye*
[4]*İstanbul Beykoz State Hospital, Clinic of Urology, İstanbul, Turkiye*
[5]*Memorial Sloan Kettering Cancer Centre, Department of Pathology, New York, USA*
[6]*İstanbul University-Cerrahpaşa, Cerrahpaşa Faculty of Medicine, Department of Urology, İstanbul, Turkiye*

Abstract

Neuroendocrine tumors (NETs) are tumors originating from neuroendocrine cells. NETs in the kidneys are extremely rare, with fewer than 100 reported cases of renal well-differentiated (WD)-NETs. A 19-year-old female patient was admitted to our clinic, with left flank pain for 2 years. Abdominal computed tomography revealed a 55x47 mm mass in the left kidney. Following a complete examination, a robot-assisted laparoscopic partial nephrectomy of the left kidney was performed under general anesthesia. The postoperative pathology indicated a WD-NET of the left kidney. The mitotic index was one per ten high power field. The Ki-67 proliferative index was found to be 6%. During the follow-up period, metastases were detected in the liver, left adrenal, right iliac crest and vertebral corpuscles, left paraaortic lymph nodes, chest, and thyroid, and different treatment regimens were applied. WD-NET is a relatively low grade malignancy, but distant metastasis can be seen. A cut-off value above 3% for Ki-67 proliferative index is considered unfavorable in patient follow-up. Somatostatin receptor scintigraphy is a valuable imaging modality for the detection and staging of recurrence or metastasis. The treatment algorithm for metastatic disease is still controversial.

Keywords: Basic science, pathology, radiology, urooncology

Introduction

Well-differentiated neuroendocrine tumors (WD-NETs) are characteristically low-grade malignant tumors that originate from neuroendocrine cells. WD-NETs most commonly occur in the gastrointestinal tract (74%) and lungs (25%) (1). WD-NETs of the urogenital tract are extremely rare, with <100 reported cases of renal NET, approximately 20 cases of bladder NET, and even fewer cases of primary urethral NET (2). Primary WD-NETs of the kidney have a median age of detection of 45 years (range: 21 to 78 years), and occur without sex predilection. As many as 15% of renal NETs have been reported in horseshoe kidneys, but no familial clustering or other associations have been noted (3). Our aim was to present a rare metastatic primary renal WD-NET case in a young female patient and to review the differential diagnosis, prognostic features, and treatment options.

Case Presentation

A 19-year-old female patient was admitted to our clinic with a 2-year history of left flank pain. She had no additional complaints and no known history of systemic disease. Importantly, she had no history of well-established risk factors associated with renal tumors, such as smoking, obesity, hypertension, or metabolic syndrome (4). Preoperative routine blood tests revealed no abnormalities. Multi-phase contrast-enhanced abdominal computed tomography (CT) demonstrated a heterogeneous soft tissue density mass, measuring approximately 55×47 mm, with

Correspondence: Bülent Önal MD, İstanbul University-Cerrahpaşa, Cerrahpaşa Faculty of Medicine, Department of Urology, İstanbul, Turkiye
E-mail: bulonal@yahoo.com **ORCID-ID:** orcid.org/0000-0003-0540-2693
Received: 09.03.2025 **Accepted:** 14.07.2025 **Epub:** 22.07.2025

Cite this article as: Aferin U, Gürses İ, Dereköylü E, Kalender G, Urgancı N, Önal B. Metastatic primary renal well-differentiated neuroendocrine tumor: our experience with current treatment and clinical management in a young female patient. J Urol Surg. [Epub Ahead of Print]

thin peripheral calcifications and exophytic extension arising from the left kidney. During the corticomedullary phase, the mass exhibited marked heterogeneous enhancement. In the nephrographic and pyelographic phases, it showed decreased density with non-enhancing necrotic areas (Figure 1).

No lymph node or distant metastasis was detected in thoracoabdominal CT. Robot-assisted laparoscopic left partial nephrectomy was performed with the prediagnosis of renal cell carcinoma. Macroscopically, a soft solid mass with well-defined borders was seen. The cross-sectional surface of the tumor was tan-brown and had a heterogeneous appearance (Figure 2). Microscopically, the tumor revealed mixed nests, anastomosing trabeculae, ribbons, and pseudo glandular growth patterns. Monotonous tumor cells had moderate amounts of eosinophilic cytoplasm and round, regular nuclei with granular, "salt and pepper" chromatin with inconspicuous nucleoli. The mitotic index was 1/10 high power field. Necrosis and lymphovascular invasion were not observed. There was extensive hemorrhage and focal areas of calcification and reactive bone formation within the tumor. Tumor cells invaded the kidney capsule in the multifocal area, but there was no extension outside the capsule. The surgical margins of the specimen were intact. Immunohistochemically, the tumor cells showed diffuse and strong staining for synaptophysin and chromogranin (Figure 3). There was no expression of cytokeratin 7 and PAX-8. Ki-67 proliferative index was determined to be 6%. The pathological diagnosis was in concordance with WD-NET, based on the 4th edition of the World Health Organization Classification of Tumors of the Urinary System and Male Genital Organs (WHO 2016) (4). Although preoperative screening for metastases with thoracoabdominal CT was conducted, no specific scan for NET was initially performed because NET was not considered. Systemic somatostatin receptor scintigraphy (SRS) performed postoperatively revealed no suspicious lesion. Serum chromogranin A (CgA) and urine 5-hydroxyindole acetic acid (5-HIAA) levels were negative. A hereditary cancer panel analysis was performed using next-generation sequencing in our patient. A pathogenic homozygous c884C>T mutation in the *MUTYH* gene was detected in another tertiary centre.

According to the decision of the multidisciplinary urooncology council (MUC), a follow-up appointment and imaging were planned in the 3rd month after surgery.

Postoperative abdominal imaging at the 3rd and 10th months was unremarkable. The patient was lost to follow-up for 19 months due to the Coronavirus disease 2019 pandemic. Abdominal magnetic resonance imaging performed 29 months after diagnosis revealed several lesions 1 cm in diameter in segments 4-5 of the liver, lesions 5 cm in diameter in the left adrenal, millimetric lesions suggestive of metastasis in the right iliac crest and vertebral corpus, and several left paraaortic lymph nodes.

Subsequently, SRS performed at the 30-month mark revealed increased activity consistent with metastatic lesions (Table 1). In accordance with the MUC's decision, tru-cut biopsies were taken from the liver and lymph node for histopathological correlation. Since the patient was young, bone biopsy was not performed to avoid affecting bone development. Biopsy results were reported as indicating metastasis of WD-NET. The mitotic index of the tumor in the lymph node was 2/10 BBA, while the Ki-67 proliferative index was 7%. Whilst the mitotic index of the tumor in the liver was 1/5BBA, and the Ki-67 proliferative index was 3% (Figure 3), further analysis is required to assess the tumor's growth potential.

Capecitabine was administered at 500 mg three times a day, temozolomide at 20 mg twice daily, octreotide at 30 mg monthly, and zoledronic acid once a month. The SRS was performed 12 months after the systemic treatment (42nd month of follow-up).

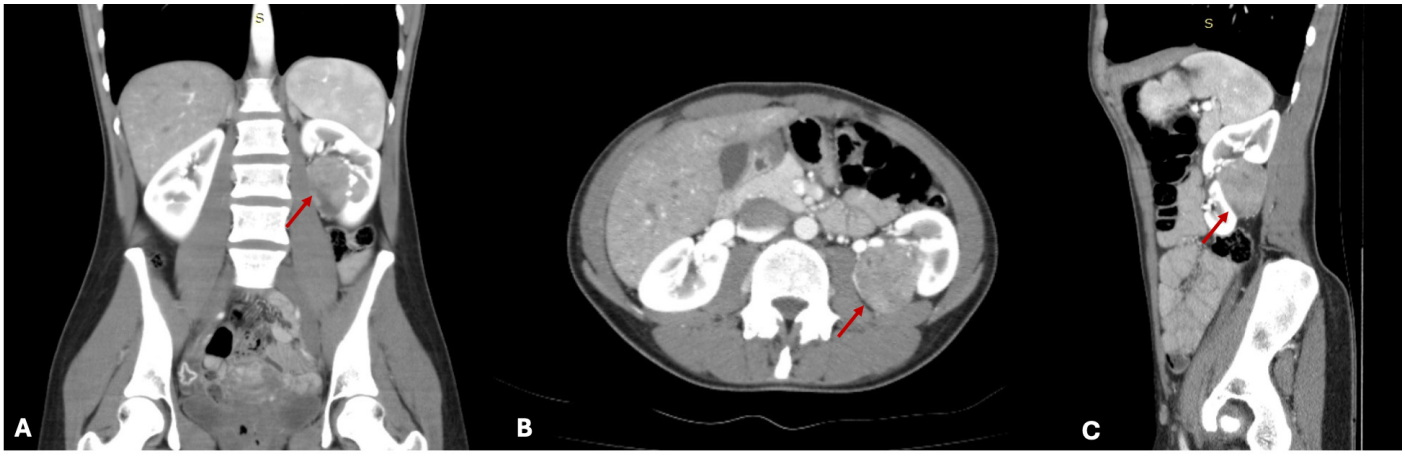

Figure 1. Coronal (A), axial (B) and sagittal (C) images obtained during the corticomedullary phase show a mass with peripheral calcifications, heterogeneous enhancement, and extension into the renal sinüs

There was an increase in the size of the lesions in the liver in Ga-68 DOTATATE uptake in lesions of adrenal glands and lymph nodes. There were multiple lytic-sclerotic bone, breast, and thyroid gland lesions with increased Ga-68 DOTATATE uptake at different intensities (Table 1).

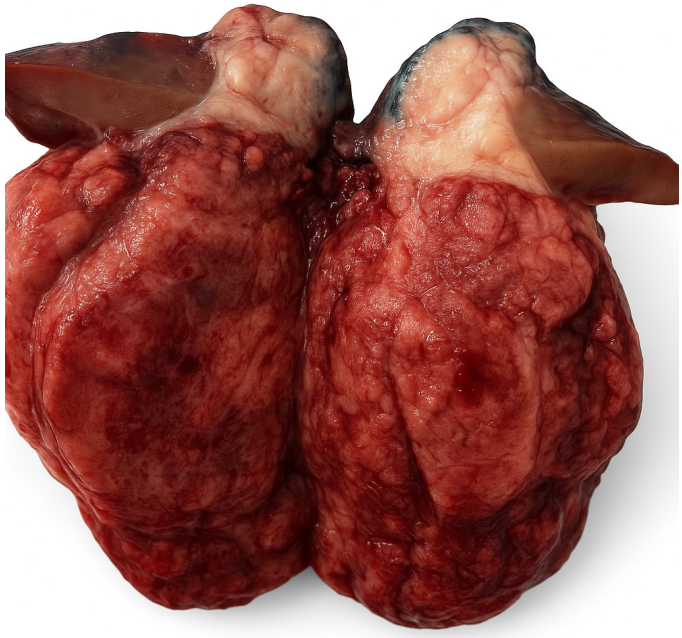

Figure 2. The macroscopic examination of the surgical specimen

Since the patient's home city was far from our hospital, a tru-cut breast biopsy has been performed by a medical oncologist at another medical center and reported as WD-NET. The mitotic index of breast tumors was 1/10 BBA, while the Ki-67 proliferative index was 4%. Due to the progression of existing metastases and detection of new metastases, capecitabine treatment was stopped and sunitinib 37.5 mg was added. Ulcers on her feet and gums developed after 6 months. The dermatological examination did not reveal the cause of the ulcers. The patient is under observation without treatment. Healing and recurrent ulcers continue to be observed.

Ga-68 DOTA-TATE scintigraphy was repeated at the 48th, 52nd, 58th, and 64th months. Treatment was managed according to the findings (Table 1). She has been suffering from bone pain despite using pain-relieving patches (transdermal fentanyl) and oral opioid analgesics. No additional clinical and laboratory findings have been observed to date. Written informed consent was obtained from the patient for their anonymized information to be published in this article.

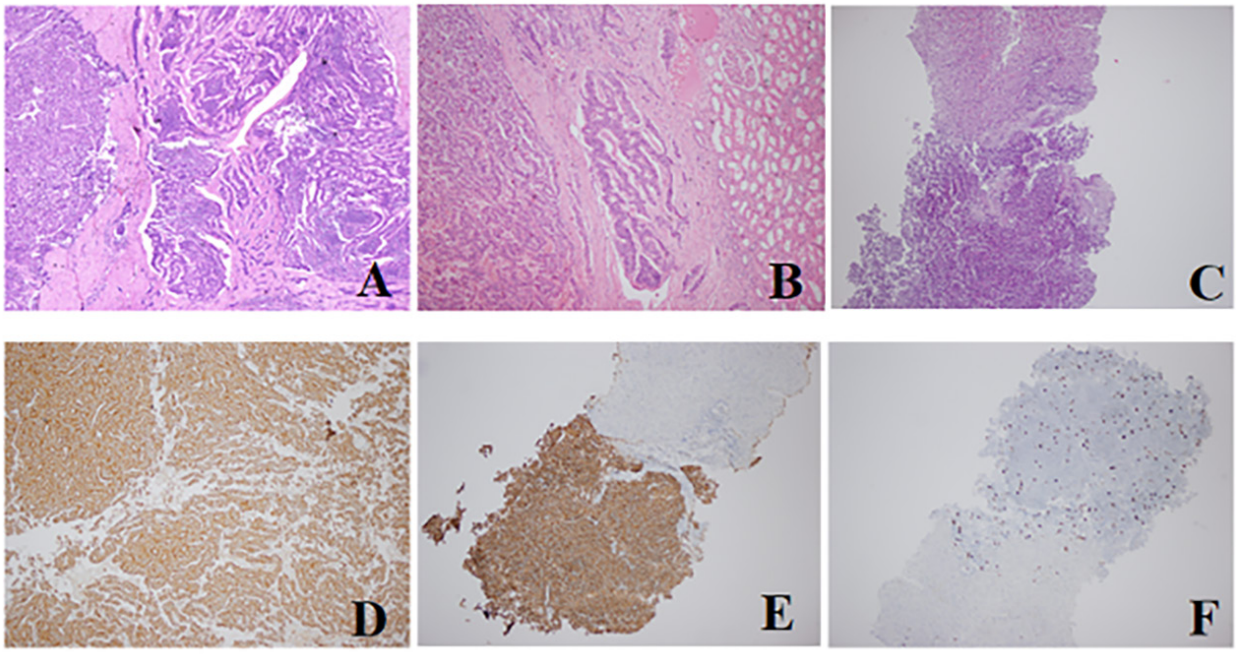

Figure 3. Well-differentiated neuroendocrine tumor of the kidney and liver metastasis: (A) The tumor revealed mixed nests, anastomosing trabeculae, ribbons, and pseudo glandular growth patterns (H&E, x20); (B) Monotonous tumor cells with typical trabecular growth pattern were well separated from the surrounding renal parenchyma (H&E, x100); (C) Histologic features of liver metastasis. The typical trabecular and sheet-like growth patterns were observed and tumor was separated from the liver tissue by a sharp border (H&E, x100); (D) Synaptophysin showed diffuse positive staining (Synaptophysin, x100); (E) Positivity of synaptophysin was observed in metastatic tumor (Synaptophysin, x100); (F) Ki-67 proliferative index of metastatic tumor was found to be 7% (Ki-67, x100)

H&E: Hematoxylin and Eosin

Table 1. Follow-up and treatment protocol and outcomes

Follow-up	Month 3	Month 10	Month 30	Month 42	Month 48	Month 52	Month 58	Month 64
Treatment protocol	Follow-up/monitoring continued		1) Capecitabine 500 mg three times a day, 2) temozolomide 20 mg twice a day, 3) Octreotide 30 mg once a month, 4) Zoledronic acid once a month treatments		1) Sunitinib 37.5 mg, 2) Temozolomide 20 mg, 3) Octreotide 30 mg, 4) Zoledronic acid		1) Sunitinib 37.5 mg, 2) Octreotide 30 mg, 3) Zoledronic acid	1) Temozolomide 70 mg, 3) Octreotide 30 mg, 4) Zoledronic acid
68Ga-DOTATATE PET/CT findings	PET was not planned because there were no MRI findings		**Liver**: Max. 1 cm in segments 4-5 (SUV_{max}=5.69)	**Liver**: Max. 2 cm in segments 4-5 (SUV_{max}=5.69)	**Liver**: Max. 2 cm in segments 4-5 (SUV_{max}=5.69)	**Liver**: Max. 2 cm in segments 4-5 (SUV_{max}=16.89)	**Liver**: Max. 2 cm in segments 4-5 (SUV_{max}=12.44)	**Liver**: Max. 2.5 cm in segments 4-5 (SUV_{max}=25.00)
			Left surrenal region: 5 cm lesion (SUV_{max}=6.36)	**Left surrenal region:** 5 cm lesion (SUV_{max}=41.25)	**Left surrenal region:** 5 cm lesion (SUV_{max}=34.59)	**Left surrenal region:** 5 cm lesion (SUV_{max}=36.12)	**Left surrenal region:** 7 cm lesion (SUV_{max}=38.79)	**Left surrenal region:** 7 cm lesion (SUV_{max}=59.75)
			Left paraaortic lymph nodes: 6 cm lesion (SUV_{max}=6.48)	**Left paraaortic lymph nodes:** 6 cm lesion (SUV_{max}=40.47)	**Left paraaortic lymph nodes:** 6 cm lesion (SUV_{max}=36.43)	**Left paraaortic lymph nodes:** 6 cm lesion (SUV_{max}=45.72)	**Left paraaortic lymph nodes:** 6 cm lesion (SUV_{max}=32.67)	**Left paraaortic lymph nodes:** 4 cm lesion (SUV_{max}=50.58)
			Right iliac crest and vertebral column: (SUV_{max}=6.99)	**Right iliac crest and vertebral column:** (SUV_{max}=6.99)	**Right iliac crest and vertebral column**	**Right iliac crest and vertebral column**	**Right iliac crest and vertebral column**	**Right iliac crest and vertebral column**
				Cranium, left scapula, left caput humerus: (SUV_{max}=7.36)	**Cranium, left scapula, left caput humerus**	**Cranium, left scapula, left caput humerus**	**Cranium, left scapula, left caput humerus**	**Cranium, left scapula, left caput humerus**
				1st, 5th, 7th, 8th costars, vertebral column: (SUV_{max}=20.15)	**1st, 5th, 7th, 8th costars, vertebral column:** (SUV_{max}=20.34)	**1st, 5th, 7th, 8th costars, vertebral column:** (SUV_{max}=27.69)	**1st, 5th, 7th, 8th costars, vertebral column:** (SUV_{max}=19.86)	**1st, 5th, 7th, 8th costars, vertebral column:** (SUV_{max}=41.13)
				Middle and left sacrum, bilateral iliac wings, bilateral acetabular posterior and proximal part of both femurs showed lytic-sclerotic bone lesions	Middle and left sacrum, bilateral iliac wings, bilateral acetabular posterior and proximal part of both femurs showed lytic-sclerotic bone lesions	Middle and left sacrum, bilateral iliac wings, bilateral acetabular posterior and proximal part of both femurs showed lytic-sclerotic bone lesions	Middle and left sacrum, bilateral iliac wings, bilateral acetabular posterior and proximal part of both femurs showed lytic-sclerotic bone lesions	Middle and left sacrum, bilateral iliac wings, bilateral acetabular posterior and proximal part of both femurs showed lytic-sclerotic bone lesions
				Right breast: 12 mm (SUV_{max}=25.53)	**Right breast:** 14 mm (SUV_{max}=22.54)	**Right breast:** 18 mm (SUV_{max}=25.10)	**Right breast:** 18 mm (SUV_{max}=25.10)	**Right breast:** 23 mm (SUV_{max}=37.86)
				The right lobe of the thyroid gland: (SUV_{max}=14.53)	**The right lobe of the thyroid gland:** (SUV_{max}=14.53)	**The right lobe of the thyroid gland:** (SUV_{max}=14.53)	**Right lobe of the thyroid gland:** (SUV_{max}=17.98)	**Right lobe of the thyroid gland:** (SUV_{max}=29.81)
							Left infraclavicular lymph node: (SUV_{max}=15.66)	**Left infraclavicular lymph node:** (SUV_{max}=35.4)

PET: Positron emission tomography, CT: Computed tomography, MRI: Magnetic resonance imaging, SUV_{max}: Maximum standard uptake value

Discussion

Urogenital system NETs are rare. According to the 5th edition of the WHO Classification of Urinary and Male Genital Tumors (WHO 2022), they are categorized into WD-NETs (grade 1 and 2), neuroendocrine carcinomas [small cell neuroendocrine carcinoma (SCNEC), large cell neuroendocrine carcinoma (LCNEC), mixed neuroendocrine neoplasm] and paragangliomas. The NETs in the kidney are extremely rare, with reported cases of <100 renal WDNET, <50 renal SCNECs, and <10 renal LCNECs (5).

In contrast to the lung, pancreas, and gastrointestinal tract, the diagnostic criteria for urogenital NETs are not well defined. According to WHO 2016, WD-NETs lacked necrosis and have low mitotic activity (<4/10BBA) (4). In the WHO 2022 classification, WD-NET was divided into grades 1 and 2. While no cut-off value for mitotic index was specified, Ki-67 proliferative index above 3% was reported as a poor prognostic parameter (5).

Primary renal WD-NET was first defined in 1966 and has been documented in case reports or short series in the literature (6). The pathogenesis of this tumor is still controversial. Neuroendocrine cells have been identified in the bladder, prostate, and renal collecting system. They are absent in the renal parenchyma. Several theories have been proposed regarding the pathogenesis: metastasis to the kidney from an unknown primary origin, intestinal metaplasia of the pyelocalyceal urothelium due to chronic inflammation, entrapped neural crest cells, and primitive stem cell differentiation (7). In addition, a loss of heterozygosity in chromosome 3p21 has been demonstrated in a subset of renal NETs, and the mutated genes were CDH1 and TET2 (8). A pathogenic homozygous c884C>T mutation in the *MUTYH* gene was detected in our patient, and she was found to be a carrier for familial adenomatous polyposis 2. No association between renal WD-NET and *MUTYH* gene mutation has been reported before. Primary renal WD-NET is associated with developmental and congenital renal diseases such as horseshoe kidneys and polycystic kidney disease. In addition, teratomas are associated with increased incidence (3,9). Our patient has no renal diseases.

WD-NETs usually occur in the renal parenchyma (92.8%) and are less common in the renal pelvis (7.2%); the right and left kidneys are involved equally. They were frequently seen after the fourth decade. Our patient is 19 years old and is considerably younger than the average. Tumors are usually solid, may contain a cystic component, or even be completely cystic. The average size is 50 mm, although sizes as large as 300 mm have been described. It is often a slow-growing, nonfunctional, and asymptomatic tumor. 25-30% of cases are diagnosed incidentally. The most common symptom is abdominal or flank pain, but abdominal, palpable mass, hematuria, constipation, and weight loss may also be observed. Carcinoid syndrome can occur in 7.1-12.7% of patients. Vasoactive substances (serotonin) produced by the tumor cause carcinoid syndrome symptoms, such as flushing and diarrhea (9). There were no signs of carcinoid syndrome in our patient.

CT is the preferred imaging method for evaluating renal masses. There are no specific findings on CT that distinguish WD-NETs from other renal masses. Tumours often present as a well-circumscribed solid mass with minimal or no enhancement on CT, but they sometimes may contain a cystic component (6,10). Different protocols for post-diagnostic follow-up are described in the literature and guidelines. According to the National Comprehensive Cancer Network, the Neuroendocrine and Adrenal Tumors Guidelines recommend multiphasic cross-sectional imaging modalities whenever possible. In metastatic WD-NETs, the frequency of imaging is established based on clinical or pathologic signs of aggressiveness (10).

SRS is a valuable imaging method for detecting and staging recurrence or metastasis. it is important for determining whether a patient may benefit from somatostatin receptor-directed therapy (11). Serum CgA and 5-HIAA levels are beneficial for postoperative follow-up. Positive SRS is more sensitive and specific than serum CgA levels in detecting metastases, but both should be considered together (10). In the follow-up of our patient, serum CgA and urine 5-HIAA levels were undetectable. There are limited data on the diagnostic value of these biomarkers in renal WD-NET. Teegavarapu et al. (9) reported increased urine 5HIAA and serum CgA levels in one case, and no distant metastasis was detected over a 52-month follow-up.

The diagnosis of NETs is based on histopathologic examination. the neuroendocrine immunophenotype was supported by strong and diffuse staining with synaptophysin, chromogranin, CD56, neuron-specific enolase, and INSM1. Calcification may present in different sizes, from small psammomatous calcification to large calcified areas (5,8).

It is hard to predict the prognosis of renal WD-NETs due to their rarity and heterogeneous behavior. It is a relatively low-grade malignancy, but local invasion, lymph node, and distant metastasis have been reported. Lymph node and liver metastases have been frequently detected. However, distant organ metastases may vary.

Stage has been shown to be the strongest predictor of outcomes. Recently, there has been an attempt to use the Ki-67 index as a prognostic marker, with 3% being a cut-off value for favorable and unfavorable behavior (5). In our case, the mitotic index of the primary tumor was 1/10BBA, while the proliferative index of Ki-67 was 6%, and metastasis occurred. Chronologically, liver, left adrenal, lymph nodes, bones and vertebral column, thyroid

gland, and breast metastases were detected. She is a unique case that has progressive distant organ metastases and develops new ones despite treatment. Liver and lymph node metastases were determined at 30 months after the operation. Therefore, long-term follow-up is necessary in this tumor.

The clinical behavior of tumors remains unclear, and management of this disease is not well established. The gold standard treatment for localized disease is partial or radical nephrectomy (6). Regional lymph node dissection should be performed if there is any suspicion of lymph node involvement (6). Surgical excision of the metastatic lesions may be performed (10). Transarterial embolization was performed in a case with extensive liver metastasis (10). Metastasis in the breast is extremely rare in WD-NETs. No case of renal WD-NET with breast metastasis has been reported in the literature. Our patient is the first reported case of breast metastasis in this specific context or population. No surgical procedure was considered due to extensive metastases. The patients continued to receive follow-up under medical therapy. Recent studies focusing exclusively on renal WD-NETs have demonstrated a generally indolent behavior and favorable prognosis, even in cases with metastatic spread. In the study by Pivovarcikova et al. (8), 3 out of 11 patients (27%) presented with metastatic disease either at the time of diagnosis or during follow-up; nonetheless, all patients were alive at a mean follow-up of 63 months (range: 12-180 months). Similarly, Jiang and Zhang (1) reported two metastatic cases (22%) among nine patients, with the liver being the predominant metastatic site. While one patient with metastasis died within three years, the remaining eight -most of whom had undergone radical nephrectomy- were alive at a mean follow-up of 37.2 months. Consistent with these findings, our patient -who developed multiple metastases during follow-up, including the liver, left adrenal gland, lymph nodes, bones, thyroid, and breast- remains alive at 64 months.

There is no consensus on the standard treatment of metastatic renal WD-NETs. Systemic chemotherapy has a limited effect in metastatic patients with low response rates (10). Somatostatin analogs and targeted therapy with tyrosine kinase inhibitors in the treatment of metastatic renal NETs are not clearly understood. WD-NETs and metastatic lesions have a high affinity for the somatostatin receptor. Somatostatin analogs are cytostatic agents against neoplastic cells (11). The PROMID study investigated the effect of octreotide, a somatostatin analog, on tumor growth in patients with metastatic midgut NETs. This study suggested that octreotide significantly prolonged the tumor progression time (12). Cases of metastatic renal WD-NETs treated with octreotide therapy have been reported (9). Sunitinib, a tyrosine kinase inhibitor, is a treatment option for treating WD-pancreatic NETs and may also have an effect against metastatic renal NETs (13). Sunitinib treatment was started in our patient who progressed under first-line treatment; however, further clinical studies are needed. Various chemotherapy regimens, including capecitabine, oxaliplatin, temozolomide, etoposide, cisplatin/carboplatin, and 5-fluorouracil, can also be utilized. Still, progression under these treatments has been reported (10,14).

Radiotherapy is a palliative treatment for the symptoms of metastatic disease and also improves the symptoms of carcinoid syndrome. Lutetium-177 dotatate is a radiolabeled somatostatin analog used as peptide receptor radionuclide therapy (PRRT). It is FDA-approved for the treatment of somatostatin receptor-positive gastroenteropancreatic NETs. There are currently no randomized data, but treatment efficacy and positive outcomes have been reported when PRRT is used for PanNETs, pheochromocytomas, paragangliomas, and bronchopulmonary/thymic NETs (15).

The treatment regimen changes made by the MUC for our patient during the follow-up period are shown in Table 1. As the patient's condition progresses, the patient will be evaluated for PRRT lutetium-177 dotatate. For lesions in the liver, liver-targeted treatment options may also be considered, such as surgical resection (which may include intraoperative thermal ablation of the lesions), hepatic arterial embolization, percutaneous thermal ablation (including bland transarterial embolization, chemoembolization, and radioembolization), and stereotactic ablative body radiotherapy.

Conclusion

Primary renal WD-NETs are extremely rare. It is a relatively low-grade malignancy, but local invasion, lymph node involvement, and distant metastasis may occur in patients. Therefore, long-term follow-up is necessary. A cut-off value above 3% for Ki-67 proliferative index is considered to be indicative of an unfavorable prognosis for patient follow-up. Serum and urine biomarkers may be negative even in metastatic cases. SRS is a valuable imaging modality for the detection and staging of recurrence or metastasis. There is no defined treatment algorithm. Partial or radical nephrectomy should be performed in localized disease. The efficacy of chemotherapy and somatostatin analogs in metastatic disease is controversial.

Ethics

Informed Consent: Written informed consent was obtained from the patient for their anonymized information to be published in this article.

Footnotes

Authorship Contributions

Surgical and Medical Practices: İ.G., B.Ö., Concept: U.A., İ.G., B.Ö., Design: U.A., İ.G., B.Ö., Data Collection or Processing: E.D., G.K., N.U., Analysis or Interpretation: U.A., E.D., G.K., Literature Search: U.A., E.D., G.K., Writing: U.A., İ.G., E.D.

Conflict of Interest: No conflict of interest was declared by the authors.

Financial Disclosure: The authors declared that this study received no financial support.

References

1. Jiang H, Zhang H. Clinical and pathological features of primary renal well-differentiated neuroendocrine tumor. Onco Targets Ther. 2022;15:587-596. [Crossref]
2. Warncke J, White S, O'Keefe M, Kim F, da Silva RD. Primary carcinoid tumor of the bladder. Can J Urol. 2018;25:9421-9423. [Crossref]
3. Krishnan B, Truong LD, Saleh G, Sirbasku DM, Slawin KM. Horseshoe kidney is associated with an increased relative risk of primary renal carcinoid tumor. J Urol. 1997;157:2059-2066. [Crossref]
4. Moch H, Cubilla AL, Humphrey PA, Reuter VE, Ulbright TM. The 2016 WHO classification of tumours of the urinary system and male genital organs-part a: renal, penile, and testicular tumours. Eur Urol. 2016;70:93-105. [Crossref]
5. Rindi G, Mete O, Uccella S, Basturk O, La Rosa S, Brosens LAA, Ezzat S, de Herder WW, Klimstra DS, Papotti M, Asa SL. Overview of the 2022 WHO classification of neuroendocrine neoplasms. endocr pathol. 2022;33:115-154. [Crossref]
6. Nguyen AH, O'Leary MP, De Andrade JP, Ituarte PHG, Kessler J, Li D, Singh G, Chang S. Natural history of renal neuroendocrine neoplasms: a NET by any other name? Front Endocrinol (Lausanne). 2021;11:624251. [Crossref]
7. Guy L, Bégin LR, Oligny LL, Brock GB, Chevalier S, Aprikian AG. Searching for an intrinsic neuroendocrine cell in the kidney. An immunohistochemical study of the fetal, infantile and adult kidney. Pathol Res Pract. 1999;195:25-30. [Crossref]
8. Pivovarcikova K, Agaimy A, Martinek P, Alaghehbandan R, Perez-Montiel D, Alvarado-Cabrero I, Rogala J, Kuroda N, Rychly B, Gasparov S, Michalova K, Michal M, Hora M, Pitra T, Tuckova I, Laciok S, Mareckova J, Hes O. Primary renal well-differentiated neuroendocrine tumour (carcinoid): next-generation sequencing study of 11 cases. Histopathology. 2019;75:104-117. [Crossref]
9. Teegavarapu PS, Rao P, Matrana M, Cauley DH, Wood CG, Tannir NM. Neuroendocrine tumors of the kidney: a single institution experience. Clin Genitourin Cancer. 2014;12:422-427. [Crossref]
10. Shah MH, Goldner WS, Benson AB, Bergsland E, Blaszkowsky LS, Brock P, Chan J, Das S, Dickson PV, Fanta P, Giordano T, Halfdanarson TR, Halperin D, He J, Heaney A, Heslin MJ, Kandeel F, Kardan A, Khan SA, Kuvshinoff BW, Lieu C, Miller K, Pillarisetty VG, Reidy D, Salgado SA, Shaheen S, Soares HP, Soulen MC, Strosberg JR, Sussman CR, Trikalinos NA, Uboha NA, Vijayvergia N, Wong T, Lynn B, Hochstetler C. Neuroendocrine and adrenal tumors, version 2.2021, NCCN clinical practice guidelines in oncology. J Natl Compr Canc Netw. 2021;19:839-868. [Crossref]
11. Hope TA, Allen-Auerbach M, Bodei L, Calais J, Dahlbom M, Dunnwald LK, Graham MM, Jacene HA, Heath CL, Mittra ES, Wright CL, Fendler WP, Herrmann K, Taïeb D, Kjaer A. SNMMI procedure standard/EANM practice guideline for SSTR PET: imaging neuroendocrine tumors. J Nucl Med. 2023;64:204-210. [Crossref]
12. Rinke A, Müller HH, Schade-Brittinger C, Klose KJ, Barth P, Wied M, Mayer C, Aminossadati B, Pape UF, Bläker M, Harder J, Arnold C, Gress T, Arnold R; PROMID Study Group. Placebo-controlled, double-blind, prospective, randomized study on the effect of octreotide LAR in the control of tumor growth in patients with metastatic neuroendocrine midgut tumors: a report from the PROMID study group. J Clin Oncol. 2009;27:4656-4663. [Crossref]
13. Raymond E, Dahan L, Raoul JL, Bang YJ, Borbath I, Lombard-Bohas C, Valle J, Metrakos P, Smith D, Vinik A, Chen JS, Hörsch D, Hammel P, Wiedenmann B, Van Cutsem E, Patyna S, Lu DR, Blanckmeister C, Chao R, Ruszniewski P. Sunitinib malate for the treatment of pancreatic neuroendocrine tumors. N Engl J Med. 2011;364:501-513. Erratum in: N Engl J Med. 2011;364:1082. [Crossref]
14. Strosberg JR, Fine RL, Choi J, Nasir A, Coppola D, Chen DT, Helm J, Kvols L. First-line chemotherapy with capecitabine and temozolomide in patients with metastatic pancreatic endocrine carcinomas. Cancer. 2011;117:268-275. [Crossref]
15. Strosberg J, El-Haddad G, Wolin E, Hendifar A, Yao J, Chasen B, Mittra E, Kunz PL, Kulke MH, Jacene H, Bushnell D, O'Dorisio TM, Baum RP, Kulkarni HR, Caplin M, Lebtahi R, Hobday T, Delpassand E, Van Cutsem E, Benson A, Srirajaskanthan R, Pavel M, Mora J, Berlin J, Grande E, Reed N, Seregni E, Öberg K, Lopera Sierra M, Santoro P, Thevenet T, Erion JL, Ruszniewski P, Kwekkeboom D, Krenning E; NETTER-1 Trial Investigators. Phase 3 trial of 177Lu-dotatate for midgut neuroendocrine tumors. N Engl J Med. 2017;376:125-135. [Crossref]